Chapter 4

Hydromagnetic oscillatory reactive flow through a porous channel in rotating frame subject to convective heat exchange under Arrhenius kinetics*

4.1 Introduction

The problems of fluid flow in a porous pipe and channel have been studied by many researchers [221-226] with a view to understanding some practical phenomena like transpiration cooling and gaseous diffusion. Particularly the pulsatile flow in a porous channel is important in the dialysis of blood in artificial kidneys [227]. The flow of electrically conducting viscous fluid between two parallel plates in the presence of a transversely applied magnetic field has applications in many devices and processes such as propulsion, plasma confinement, MHD power generators, MHD pumps, accelerators, aerodynamics heating, electrostatic precipitation, polymer technology, petroleum industry, cooling of nuclear reactors, geothermal energy extraction and metal purification. Hydromagnetic principles

*Published in **Journal of Engineering Physics and Thermophysics, 94(3)(2021), pp.722-733.***

is used to design heat exchangers, liquid metal pumps, microfluidic pumps, control and re-entry problems, accelerators and flow-meters, in solving space vehicle propulsion, in developing confinement schemes for controlled nuclear fusion and in creating novel electric current generating systems. A survey of MHD studies in the technological fields can be found in Moreau [228]. Hartmann [3] has carried out a pioneer work of Hartmann flow which is regarded as the source of MHD channel flow. He has examined flow of a viscous incompressible electrically conducting fluid within a parallel plate channel in the presence of a transverse magnetic field. Many varieties of important experimental, analytical and numerical studies as regards flow of a conductive fluid in between two parallel plates in the presence of a transverse magnetic field are found in the literatures [229-231] based on the work of Hartmann. The study of fluid flow and heat transfer in a porous channel have received considerable attention during the last several decades due to their relevance in a wide range of biological and engineering setting such as irrigation and drainage problems, absorption and filtration process in chemical engineering and ground water hydrology. Comprehensive reviews of magnetohydrodynamic flow and heat transfer under various physical situations can be found in [232-244].

The phenomenon of rotation has its numerous applications in cosmic and geophysical flows. Moreover, occurrence of rotation also helps in better understanding the behaviour of ocean circulation and galaxies formation. In the presence of a magnetic field, the rotating flow of an electrically conducting fluid is encountered in geophysical fluid dynamics. It is important in the solar physics dealing with the sunspot development, the solar cycle and the structure of rotating magnetic stars [245]. The effect of the Coriolis force due to the earth's rotation is found to be significant as compared to the inertial and viscous forces in the equations of motion. The Coriolis and the electromagnetic forces are of comparable magnitude. The Coriolis force exerts a strong influence on the hydromagnetic flow in the earth's liquid core which plays an important role in the mean geomagnetic field. Since most cosmic bodies are rotators, the study of rotating electrically conducting fluid is essential in understanding better the magnetohydrodynamics of the interiors of the Earth and other planets. In particular, rotating MHD flows with heat transfer is one of the important current topics because of its applications in thermofluid transport modeling in magnetic geosystems, meteorology,

turbo machinery, solidification processes in metallurgy and in some astrophysical problems. Other engineering applications include vertex MHD power generator, rotating drum type separator in a closed cycle, two phase power generator, isotopes separation, plasma diagnostics, hypersonic ionized boundary layers, particle deposition in electrically conducting systems and liquid metal processing, MHD bearings. Rotation also helps in the measurement of the energies of transitions between quantized rotational states of molecules in the gas phase (rotational spectroscopy). There are many experimental and theoretical studies on the hydromagnetic rotating flow of viscous electrically conducting fluid in different geometries [246-262].

The motion of viscous reactive fluid through channels or ducts under the effects of magnetic field is an important subject in the field of chemical, biomedical sciences and environmental engineering. This phenomenon is fundamental in nature and is of great practical importance in many diverse applications, including the production of oil and gas from geological structures, the gasification of coal, the retorting of shale oil, filtration, groundwater movement, regenerative heat exchange, surface catalysis of chemical reactions, absorption, coalescence, drying, ion exchange and chromatography. Furthermore, hydromagnetic reactive flows are often accompanied with heat transfer in many industrial and engineering applications, for instance in thermo-hydrodynamic lubrication of rotating thrust bearings [263, 264]. Makinde [265] has obtained the steady-state solutions of a strongly exothermic reaction of a viscous combustible material in a channel filled with a saturated porous medium under Arrhenius kinetics, neglecting reactant consumption. The steady flow of a reactive variable viscosity fluid in a cylindrical pipe with an isothermal wall has been presented by Makinde [266]. Makinde [267] has investigated the thermal stability of a reactive third grade fluid flowing steadily through a cylindrical pipe with isothermal wall. The thermal stability of a reactive third-grade liquid flowing steadily between two parallel plates with symmetrical convective cooling at the walls has been investigated by Makinde [268]. He has observed that a combined increase in non-Newtonian parameter and convective cooling enhances the thermal stability of the material. Makinde and Bég [269] have studied the inherent irreversibility and thermal stability in a reactive electrically conducting fluid flowing steadily through a channel with isothermal walls under the influence of a transversely imposed magnetic field.

Kobo and Makinde [270] have discussed the inherent irreversibility associated with the Couette flow of a reacting variable viscosity combustible material under Arrhenius kinetics. An unsteady hydromagnetic generalized Couette flow of a reactive third-grade fluid with asymmetric convective cooling has been presented by Makinde and Chinkyoka [271]. Makinde and Franks [272] have studied the MHD unsteady reactive Couette flow with heat transfer and variable properties. The steady generalized axial Couette flow of Ostwald-de Waele power law reactive fluids between concentric cylindrical pipes has been investigated by Makinde [273]. Srinivas [274] has examined the thermal-diffusion and chemical reaction effects on MHD pulsating flow in a porous channel with slip and convective boundary conditions. Rundora and Makinde [275] have examined the thermal effects in an unsteady hydromagnetic flow of a pressure-driven, reactive, variable viscosity, electrically conducting third-grade fluid through a porous saturated medium with asymmetrical convective boundary conditions. They have observed that the thermal critical values of the reaction parameter increase with the magnetic field intensity and the tortuosity of the porous medium.

The above literature review reveals that no study exists that investigates the combined effects of rotational force, convective heating, exothermic chemical reaction on MHD channel flow. To date, a pressure-driven laminar flow of a reactive viscous fluid confined in a channel with porous walls in a rotating environment has not been analyzed. The main objective here is to develop a model with which to determine the flow dynamics of a reactive fluid through a channel with porous walls subject to asymmetrical convective heat exchange under the effects of magnetic field and Arrhenius kinetics in a rotating frame. A convective boundary condition is used rather than the customary conditions for temperature. It is assumed that the system exchange heat with the ambient following Newton's cooling law and the reaction is exothermic under Arrhenius kinetics, neglecting the consumption of the material. Closed form solution has been obtained for the fluid velocity and temperature. The heat transfer characteristic has also been studied by taking viscous and Joule dissipations and exothermic chemical reaction function into account. In our study, the nonlinearity arises in energy equation due to the viscous and Joule heating and Arrhenius kinetic. This nonlinear energy equation can be solved numerically with the help of MATLAB software package pdepe. Numerical results are presented and discussed with respective to the per-

tinent parameters. After an exhaustive literature survey, we have found that no prior work has dealt with the problem considered here.

4.2 Formulation of the problem and its solutions

Consider an unsteady flow of a viscous incompressible electrically conducting reactive fluid placed between two infinite horizontal parallel porous plates separated by a distance a. A Cartesian co-ordinates system with the x-axis along the lower plate of the channel, y-axis normal to the channel and z-axis perpendicular to xy-plane is introduced(see Fig.4.1). The fluid and the channel are in a rigid body rotation with a uniform angular velocity Ω about the y-axis. The plate surfaces are subjected to asymmetric convective heat exchange with the ambient due to

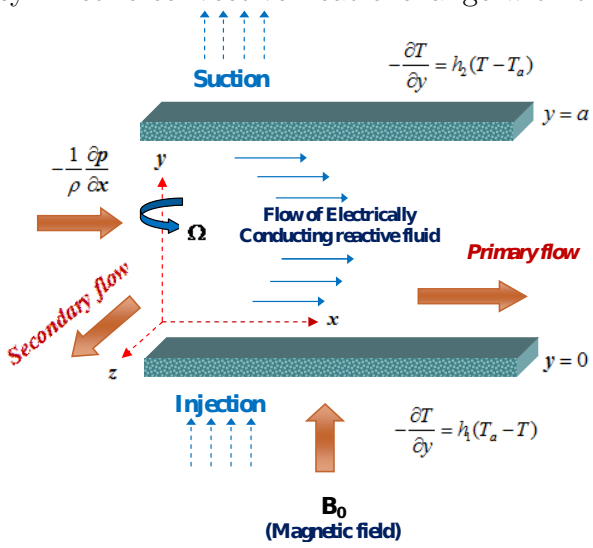

Fig.4.1: *Physical configuration*

unequal heat transfer coefficients. The flow is subjected to the influence of an applied uniform transverse magnetic field of strength B_0, which is imposed perpendicular to the channel. There is no applied voltage and the magnetic Reynolds number is small, hence the induced magnetic field and Hall effects are negligible. The fluid motion is driven by the oscillating pressure gradient. We assume an Arrhenius rate law for the chemical kinetics and hence the rate of chemical reaction increases exponentially with the absolute temperature. Since channel walls are of infinite extent in x- and z- directions, all physical quantities in the system, except pressure, are the functions of y and t only.

The equation of continuity $\nabla \cdot \vec{q} = 0$ gives $v = -v_0$ everywhere in the fluid, where $\vec{q} \equiv (u, v, w)$ is the fluid velocity vector and v_0 the uniform suction/injection velocity at the channel walls ($v_0 < 0$ implies fluid injection into lower plate and suction out of upper plate of the channel, the opposite scenario is the case when $v_0 > 0$). It is assumed that amount of the mass injection into the channel equals that of the mass suction at the opposite wall of the channel. In other words, velocities of the mass injection and suction at the plates are equal to one another. It is also assumed that the suction/injection velocity is not strong enough to significantly alter the predominantly unidirectional flow (parallel to the x- direction). Within the framework of above assumptions and neglecting the reacting viscous fluid consumption, the governing equations for the momentum and heat balance of a viscous electrically conducting reactive fluid through a channel in a rotating frame of reference on taking viscous and Joule dissipations into account are [248, 250, 261, 275]

$$\frac{\partial u}{\partial t} - v_0 \frac{\partial u}{\partial y} + 2\Omega w = -\frac{1}{\rho}\frac{\partial p}{\partial x} + \nu \frac{\partial^2 u}{\partial y^2} - \frac{\sigma B_0^2}{\rho} u, \tag{4.1}$$

$$\frac{\partial w}{\partial t} - v_0 \frac{\partial w}{\partial y} - 2\Omega u = \nu \frac{\partial^2 w}{\partial y^2} - \frac{\sigma B_0^2}{\rho} w, \tag{4.2}$$

$$\begin{aligned} \rho c_p \left(\frac{\partial T}{\partial t} - v_0 \frac{\partial T}{\partial y} \right) &= k \frac{\partial^2 T}{\partial y^2} + \mu \left[\left(\frac{\partial u}{\partial y} \right)^2 + \left(\frac{\partial w}{\partial y} \right)^2 \right] \\ &+ \sigma B_0^2 \left(u^2 + w^2 \right) + Q C_0 A_0 \, e^{-\frac{E}{RT}}, \end{aligned} \tag{4.3}$$

where u and w are the velocity components in the x- and z-direction, respectively, T the fluid temperature, t the time, p the modified fluid pressure including centrifugal force, ρ the fluid density, μ the coefficient of viscosity, σ the electrical conductivity, ν the kinematic viscosity, k the thermal conductivity, c_p the specific heat at constant pressure, Q the heat of reaction, C_0 the initial concentration of the reactant species, A_0 the rate constant, E the activation energy, R the universal gas constant.

The first term of right hand side in (4.3) is stands for heat conduction, the second term for viscous dissipation, third term for Joule heating and fourth term for the chemical reaction kinetic function in Arrhenius type. For the analysis of heat transfer characteristics in the flow, energy equation is taken in which all the convective terms become equal to zero because of the assumed temperature

boundary conditions. Therefore, the temperature distribution in the rotating channel is due to the heat generation by viscous and Joule dissipations and conduction through the fluid in the transverse direction. In many industrial and geophysical flows viscous dissipation effects may also arise owing to internal friction in viscous fluids which can affect temperature fields. Joule heating is the predominant heat mechanism for heat generation in integrated circuits and is an undesired effect. Joule heating effects are also important and are caused by heating of the electrically conducting fluid by the electrical current. The effect of Joule heating is usually characterized by the product of the magnetic parameter and Brinkman number and it has a very important part in geophysical flows and in nuclear engineering [242].

The appropriate initial and boundary conditions for the problem are given by [275]

$$u(y,0) = w(y,0) = 0, \quad T(y,0) = T_0 \quad \text{for} \quad 0 \leq y \leq a, \tag{4.4}$$

$$u(0,t) = w(0,t) = 0, \quad -k\frac{\partial T}{\partial y}(0,t) = h_1[T_a - T(0,t)], \tag{4.5}$$

$$u(a,t) = w(a,t) = 0, \quad -k\frac{\partial T}{\partial y}(a,t) = h_2[T(a,t) - T_a], \tag{4.6}$$

where h_1 and h_2 are the heat transfer coefficients at the lower and upper plates, respectively, T_0 the initial fluid temperature, T_a the ambient temperature. The lower and upper plates are cooled by convection. The coolant ambient temperature T_a is the same for both plates but the convection heat transfer coefficients h_1 and h_2 are different, thus providing an asymmetric cooling effect. The lower and upper plates of the channel are convectively heated with hot fluid at temperature T_a with heat transfer coefficient h_1 and h_2, respectively. Heat transfer with convective boundary condition is more general and realistic especially with respect to various engineering and industrial processes including material drying [276], laser pulse heating [277] and transpiration cooling [278].

Introducing the following dimensionless variables

$$\eta = \frac{y}{a}, (u_1, w_1) = \frac{(u,w)a}{\nu}, \tau = \frac{\nu t}{a^2}, \quad \theta = \frac{E(T - T_0)}{RT_0^2} \tag{4.7}$$

equations (4.1)-(4.3) can be written in dimensionless form as

$$\frac{\partial u_1}{\partial \tau} - Re\frac{\partial u_1}{\partial \eta} \quad = \quad P + \frac{\partial^2 u_1}{\partial \eta^2} - M^2\, u_1 - 2K^2 w_1, \tag{4.8}$$

$$\frac{\partial w_1}{\partial \tau} - Re\frac{\partial w_1}{\partial \eta} = \frac{\partial^2 w_1}{\partial \eta^2} - M^2\, w_1 + 2K^2 u_1, \tag{4.9}$$

$$\begin{aligned}\frac{\partial \theta}{\partial \tau} - Re\frac{\partial \theta}{\partial \eta} &= \frac{1}{Pr}\frac{\partial^2 \theta}{\partial \eta^2} + Ec\left[\left(\frac{\partial u_1}{\partial \eta}\right)^2 + \left(\frac{\partial w_1}{\partial \eta}\right)^2\right] \\ &+ M^2\, Ec\left(u_1^2 + w_1^2\right) + \delta \exp\left(\frac{\theta}{1+\alpha\theta}\right),\end{aligned} \tag{4.10}$$

where $M^2 = \frac{\sigma B_0^2 a^2}{\nu\rho}$ is the squared-Hartmann number which is representing the relative magnitude of hydromagnetic drag force and viscous hydrodynamic, $P = \frac{a^3}{\rho\nu^2}\left(-\frac{\partial p}{\partial x}\right)$ the non-dimensional axial pressure gradient, $Re = \frac{v_0 a}{\nu}$ the suction/ injection Reynolds number (or the cross flow Reynolds number), $K^2 = \frac{\Omega a^2}{\nu}$ the rotation parameter which is the reciprocal of Ekmann number, $Ec = \frac{E\nu^2}{RT_0^2 a^2 c_p}$ is the Eckert number which defines the ratio of the kinetic energy of the flow to the enthalpy difference i.e. the degree of mechanical energy dissipated as heat via internal friction, $Pr = \frac{\mu c_p}{k}$ the Prandtl number which defines the relative effectiveness of momentum and energy transport by diffusion i.e. the ratio of momentum to thermal diffusivity in fluid, $\alpha = \frac{RT_0}{E}$ the activation energy parameter, $\delta = \frac{EQC_0A_0a^2}{RT_0^2 k}\, e^{-\frac{E}{RT_0}}$ the Frank-Kamenetskii parameter or reaction rate parameter.

The corresponding non-dimensional initial and boundary conditions are

$$u_1(\eta, 0) = w_1(\eta, 0) = 0, \quad \theta(\eta, 0) = 0 \quad \text{for } 0 \le \eta \le 1, \tag{4.11}$$

$$u_1(0, \tau) = w_1(0, \tau) = 0, \quad \frac{\partial \theta}{\partial \eta}(0, \tau) = -Bi_1[\theta_a - \theta(0, \tau)], \tag{4.12}$$

$$u_1(1, \tau) = w_1(1, \tau) = 0, \quad \frac{\partial \theta}{\partial \eta}(1, \tau) = -Bi_2[\theta(1, \tau) - \theta_a], \tag{4.13}$$

where $Bi_1 = \frac{a\,h_1}{k}$ and $Bi_2 = \frac{a\,h_2}{k}$ are the Biot numbers or surface convection parameters, $\theta_a = \frac{E(T_a - T_0)}{RT_0^2}$ the ambient temperature parameter.

It is convenient to combine equations (4.8) and (4.9) into a single equation. We multiply equation (4.9) by i and add the resultant to equation (4.8) to obtain

$$\frac{\partial q}{\partial \tau} - Re\frac{\partial q}{\partial \eta} = \frac{\partial^2 q}{\partial \eta^2} - (M^2 - 2i\,K^2)\, q + P, \tag{4.14}$$

where $q(= u_1 + i\, w_1)$ is the fluid velocity in the complex form and $i = \sqrt{-1}$.

In order to solve the equation(4.14), we assume the oscillatory pressure gradient and the complex velocity in the following form

$$P = \frac{a^3}{\rho\nu^2}\left(-\frac{\partial p}{\partial x}\right) = \lambda\left[1+\frac{\varepsilon}{2}\left(e^{i\,n\,\tau}+e^{-i\,n\,\tau}\right)\right], \tag{4.15}$$

$$q(\eta,\tau) = q_0(\eta)+\varepsilon[q_1(\eta)e^{i\,n\,\tau}+q_2(\eta)e^{-i\,n\,\tau}], \tag{4.16}$$

where n is the non-dimensional frequency of pressure oscillation, λ is a known constant, $\varepsilon(\ll 1)$ is a suitable chosen positive quantity and $q_0(\eta)$, $q_1(\eta)$ and $q_2(\eta)$ are non-dimensional functions.

On the use of (4.15) and (4.16), equation (4.14) yields

$$q_0''(\eta)+Re\,q_0'(\eta)-(M^2-2\,i\,K^2)q_0(\eta)=-\lambda, \tag{4.17}$$

$$q_1''(\eta)+Re\,q_1'(\eta)-[M^2-i\,(2K^2-n)]q_1(\eta)=-\frac{\lambda}{2}, \tag{4.18}$$

$$q_2''(\eta)+Re\,q_2'(\eta)-[M^2-i\,(2K^2+n)]q_2(\eta)=-\frac{\lambda}{2}, \tag{4.19}$$

where prime denotes the differentiation with respect to η.

The boundary conditions for $q_0(\eta)$, $q_1(\eta)$ and $q_2(\eta)$ are

$$\begin{aligned} &q_0=q_1=q_2=0 \ \text{ at } \ \eta=0,\\ &q_0=q_1=q_2=0 \ \text{ at } \ \eta=1. \end{aligned} \tag{4.20}$$

Solutions of the ordinary differential equations (4.17)-(4.19) subject to the boundary conditions (4.20) are obtained as

$$q_0(\eta)=e^{-\frac{Re}{2}\eta}\,(c_1\sinh m_1\eta-c_2\cosh m_1\eta)+c_2, \tag{4.21}$$

$$q_1(\eta)=e^{-\frac{Re}{2}\eta}\,(c_3\sinh m_2\eta-c_4\cosh m_2\eta)+c_4, \tag{4.22}$$

$$q_2(\eta)=e^{-\frac{Re}{2}\eta}\,(c_5\sinh m_3\eta-c_6\cosh m_3\eta)+c_6, \tag{4.23}$$

where m_1, m_2, m_3 and $c_1, c_2, c_3, c_4, c_5, c_6$ are given as follows:
$m_1=\alpha_1-i\,\beta_1$, $m_2=\alpha_2\mp i\,\beta_2$(according as $2K^2>n$ or $2K^2<n$), $m_3=\alpha_3-i\,\beta_3$,

$$c_1=\frac{\lambda(M^2+2\,i\,K^2)}{(M^4+4\,K^4)}\left(\frac{\cosh m_1-e^{\frac{Re}{2}}}{\sinh m_1}\right),\ c_2=\frac{\lambda(M^2+2\,i\,K^2)}{(M^4+4\,K^4)},$$

$$c_3=\frac{\lambda\{M^2+i(2\,K^2-n)\}}{2\{M^4+(2\,K^2-n)^2\}}\left(\frac{\cosh m_2-e^{\frac{Re}{2}}}{\sinh m_2}\right),\ c_4=\frac{\lambda\{M^2+i(2\,K^2-n)\}}{2\{M^4+(2\,K^2-n)^2\}},$$

$$c_5 = \frac{\lambda\{M^2 + i(2\,K^2 + n)\}}{2\{M^4 + (2\,K^2 + n)^2\}} \left(\frac{\cosh m_3 - e^{\frac{Re}{2}}}{\sinh m_3} \right), c_6 = \frac{\lambda\{M^2 + i(2\,K^2 + n)\}}{2\{M^4 + (2\,K^2 + n)^2\}},$$

$$\alpha_1, \beta_1 = \frac{1}{2\sqrt{2}} \left[\{(Re^2 + 4\,M^2)^2 + 64\,K^4\}^{\frac{1}{2}} \pm (Re^2 + 4\,M^2) \right]^{\frac{1}{2}},$$

$$\alpha_2, \beta_2 = \frac{1}{2\sqrt{2}} \left[\{(Re^2 + 4\,M^2)^2 + 16(2\,K^2 - n)^2\}^{\frac{1}{2}} \pm (Re^2 + 4\,M^2) \right]^{\frac{1}{2}},$$

$$\alpha_3, \beta_3 = \frac{1}{2\sqrt{2}} \left[\{(Re^2 + 4\,M^2)^2 + 16(2\,K^2 + n)^2\}^{\frac{1}{2}} \pm (Re^2 + 4\,M^2) \right]^{\frac{1}{2}}. \quad (4.24)$$

On the use of (4.21)-(4.23), the equation (4.16) gives the solution for complex fluid velocity as

$$\begin{aligned} q(\eta, \tau) &= \{e^{-\frac{Re}{2}\eta} (c_1 \sinh m_1\eta - c_2 \cosh m_1\eta) + c_2\} \\ &+ \varepsilon \left[e^{i\,n\tau} \{e^{-\frac{Re}{2}\eta} (c_3 \sinh m_2\eta - c_4 \cosh m_2\eta) + c_4\} \right. \\ &+ \left. e^{-i\,n\tau} \{e^{-\frac{Re}{2}\eta} (c_5 \sinh m_3\eta - c_6 \cosh m_3\eta) + c_6\} \right]. \end{aligned} \quad (4.25)$$

Equation (4.25) represents the unified expression for fluid velocity of electrically conducting reactive fluid through a porous channel in rotating frame in the presence of transverse magnetic filed and uniform suction or injection at channel walls. On separating into a real and imaginary parts, one can easily obtain the velocity components u_1 and w_1 from equation (4.25).

The analytical expression of the complex velocity given by (4.25) is used in (4.10) and the resulting nonlinear partial differential equation subject to the asymmetric convective boundary conditions (4.12) and (4.13) is solved. The mechanics of nonlinear flows presents a special challenge to engineers, physics and mathematicians since the nonlinearity can manifest itself in a variety of ways as is the case in the analysis of a reactive viscous fluid flow in a channel with wall suction/ injection. This can be solved numerically using pdepe MATLAB's subroutine following Skeel and Berzins [279].

In order to validate the results of the present study, we have considered the special case. In an inertial frame of reference ($K^2 = 0$) and absence of magnetic filed ($M^2 = 0$), the solution for fluid velocity given by (4.25) reduce to those of Radhakrishnamacharya and Maiti [226] with slight changes of notations.

4.3 Results and discussion

In order to gain a physical insight into the dynamics of this physical problem, numerical computations for the velocity field, temperature field, wall shear stress and rate of heat transfer have been carried out by assigning some arbitrary chosen specific values to various embedded parameters, viz. $M^2 = 5$, $K^2 = 5$, $Re = 1$, $Pr = 0.72$, $Ec = 0.1$, $\delta = 0.1$, $\alpha = 0.1$, $\lambda = 1$, $n = 2$, $n\tau = \pi/4$ for controlling the flow system.

4.3.1 Primary and secondary velocity profiles

Fig.4.2 is plotted to illustrate the effects of various physical parameters on the primary and secondary velocity profiles across the channel. Fig.4.2(a) and 4.2(b) show the influence of squared-Hartmann number M^2 on the primary and secondary velocity profiles. Both the primary and secondary profiles are seen to decrease with an increase in M^2. An increase in squared-Hartmann number means an increase in the damping properties of the magnetic field and these damping forces result in increased resistance to flow and fluid velocity components decrease. The peak velocity occurs near the centreline ($\eta = 0.5$) of the channel and its location is virtually unaffected by the gaining strength of magnetic field. Effects of rotation parameter K^2 on primary and secondary velocity profiles within

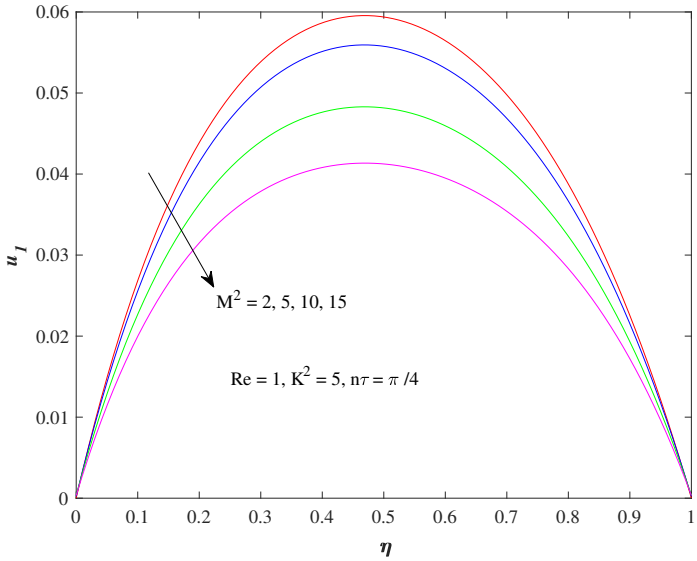

Fig.4.2(a): *Primary velocity profiles u_1-profiles varying M^2*

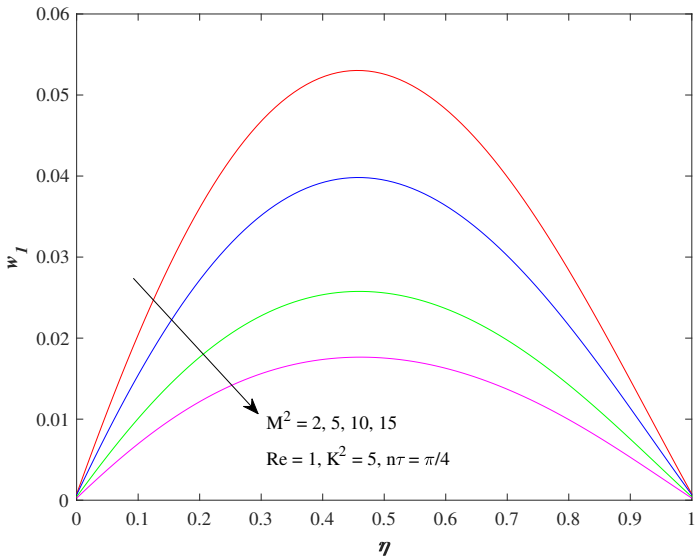

Fig.4.2(b): *Secondary velocity profiles* w_1 *varying* M^2

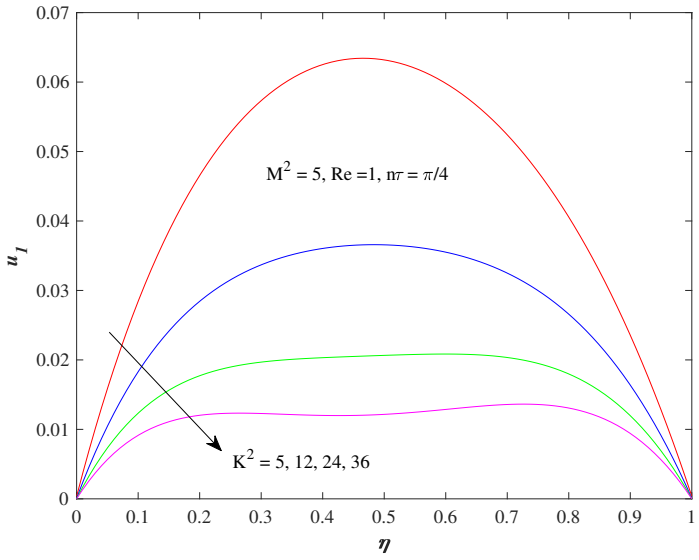

Fig.4.2(c): *Primary velocity profiles* u_1 *varying* K^2

the channel is illustrated in Figs.4.2(c) and 4.2(d). In Fig.4.2(c), the primary velocity is observed to decrease with increasing K^2. The secondary velocity increases until it reaches maximum and then decreases as K^2 increases (Fig.4.2(d)). This means that the rotation has retarding influence on the primary velocity profiles. Ekman number expresses the relative significance of viscous hydrodynamic and rotational (Coriolis) forces. The rotation parameter K^2 is inversely propor-

tional to Ekman number. For $K^2 = 1$, the viscous and rotational forces are of same order of magnitude. For $K^2 > 1$, the rotational effects clearly dominate viscous effects. For $K^2 < 1$, the rotational effects are dominated by viscous effects. Coriolis body forces arise in both the primary and secondary momentum equations. Large values of Ekman number imply lesser rotational effects on the flow field. The rotational drag force is a positive body force which has significant

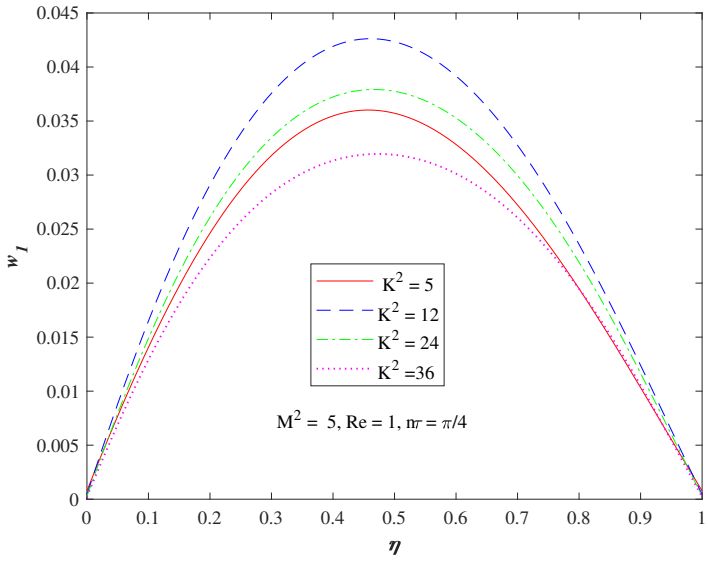

Fig.4.2(d): *Secondary velocity profiles* w_1 *varying* K^2

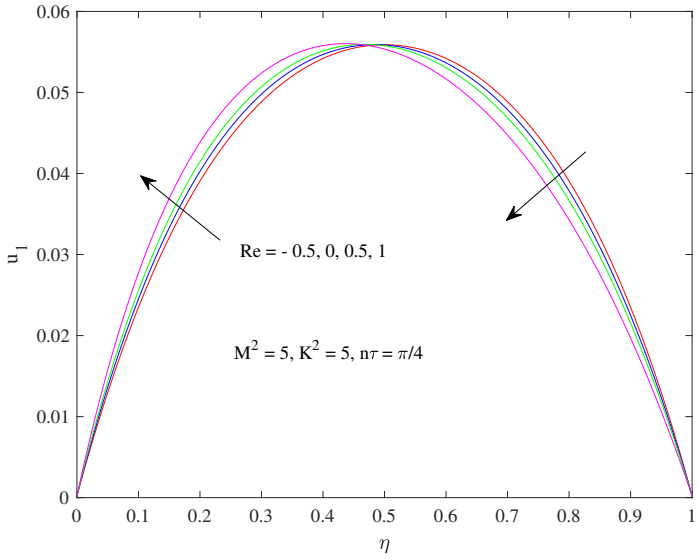

Fig.4.2(e): *Primary velocity profiles* u_1 *varying* Re

influence on flow dynamics. Figs.4.2(e) and 4.2(f) portray the effects of suction/injection on the primary and secondary velocity profiles. It is found that both velocity profiles enhance in a region near to the lower plate of the channel and results reverse in a region near to upper plate of the channel for increasing values of suction/injection parameter. The result shows that an increase in the suction/injection parameter breaks the symmetric nature of the flow due to

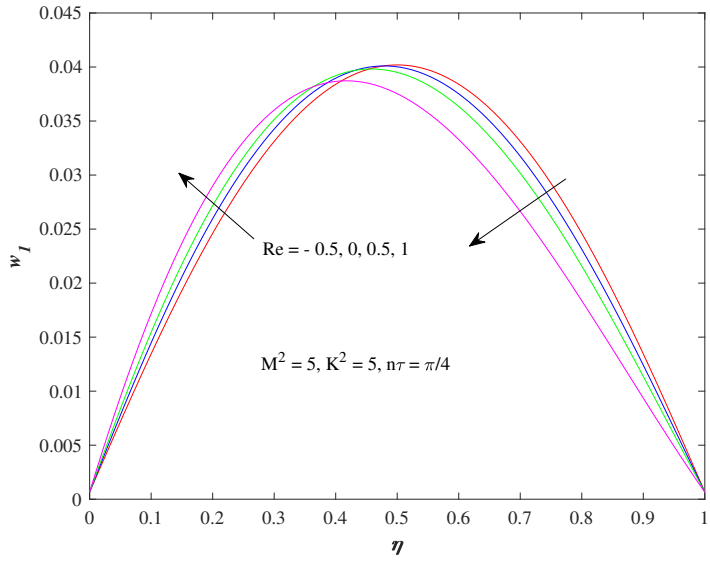

Fig.4.2(f): *Secondary velocity profiles w_1 varying Re*

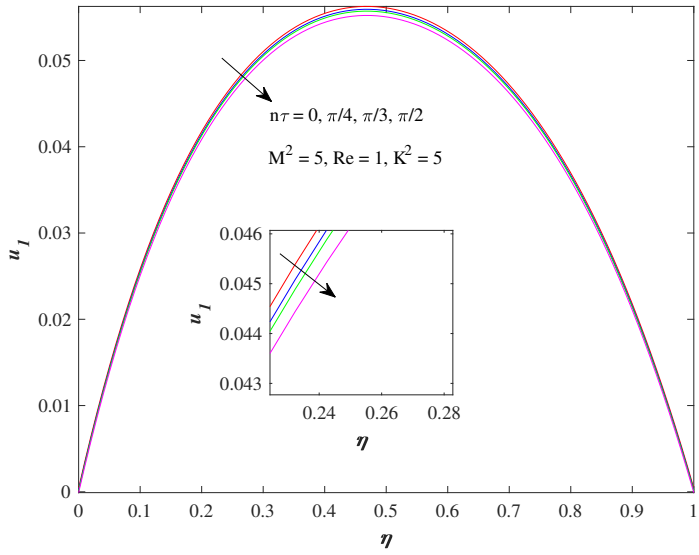

Fig.4.2(g): *Primary velocity profiles u_1 varying $n\tau$*

continual increase in the injection at the lower plate which is sucked off at the upper plate. Due to break in symmetry, the fluid flow is observed to be skewed towards the plates with suction/injection. It is interesting to note the shift in symmetry as the suction parameter increases. Figs.4.2(g) and 4.2(h) reveal that both the primary and secondary velocity profiles slightly reduce with an increase in phase angle $n\tau$.

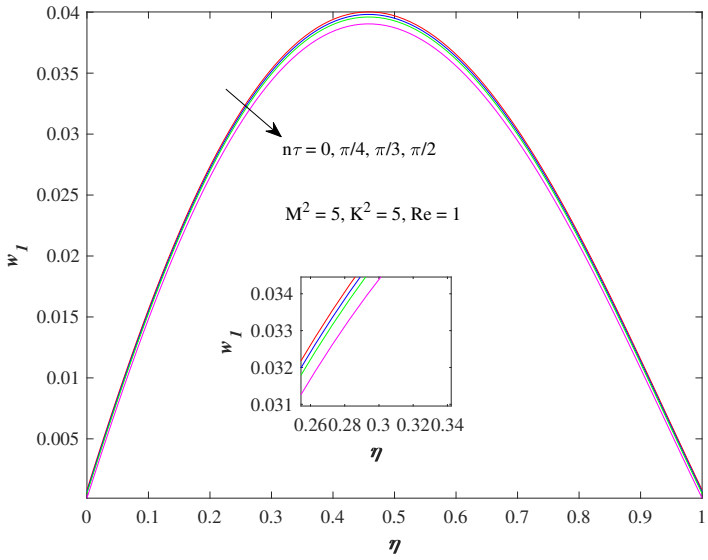

Fig.4.2(h): *Secondary velocity profiles w_1 varying $n\tau$*

4.3.2 Temperature profiles

Fig.4.3 show the behaviour of fluid temperature profiles across the channel in response to varying values of suction parameter Re, Prandtl number Pr, Eckert number Ec, reaction parameter δ, Biot numbers Bi_1, Bi_2 and time τ. Fig.4.3(a) depicts that fluid temperature profiles increase with increasing suction/injection Reynolds number Re, when all other parameter values are fixed. For uniform suction through the upper plate, increasing suction Reynolds number causes an increase in the fluid temperature due to an decrease in the rate of heat transfer across the upper plate of the channel. The result shows that as more and more hot fluid is injected into the channel, the fluid temperature within the channel increases. The effects of Prandtl number Pr on the temperature profiles in the asymmetrically cooled channel are shown in Fig.4.3(b). Temperature profiles de-

crease through out the region of the channel for increasing values of Pr. The Prandtl number tends to decrease the strength of the heating source terms in the energy equation and hence in turn reduces the fluid temperature. Fluid temperature is high near the upper plate compared to the lower plate of the channel. This is due to the asymmetric convective heating at the channel walls. Fig.4.3(c) highlights the temperature profiles for variation of Eckert number Ec within the channel. The increase of Ec is observed to be proportional to the rise in temp-

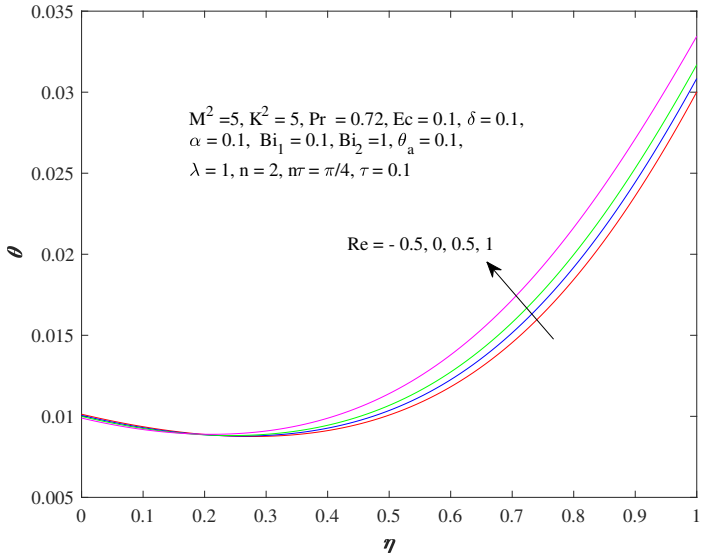

Fig.4.3(a): *Temperature profiles varying Re*

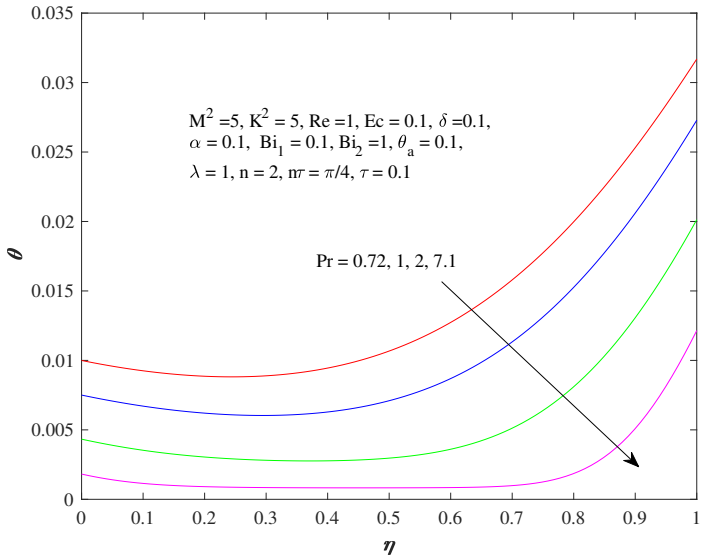

Fig.4.3(b): *Temperature profiles varying Pr*

erature profiles. As Eckert number increases, it implies higher viscous dissipation in the flow, which in turn increases the fluid temperature. The positive Eckert number means cooling of the channel walls i.e loss of heat from the channel wall to the ambient fluid. Hence, greater viscous dissipative heat causes a rise in the fluid temperature in channel. For the case of $Ec \to 0$, both viscous heating and

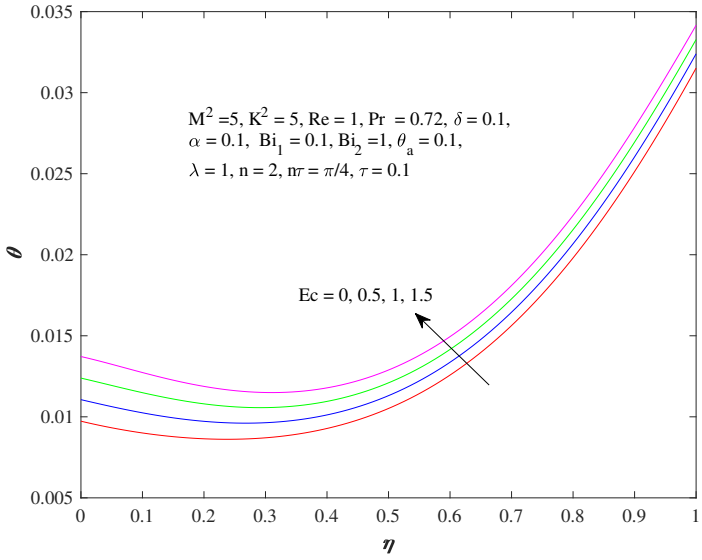

Fig.4.3(c): *Temperature profiles varying Ec*

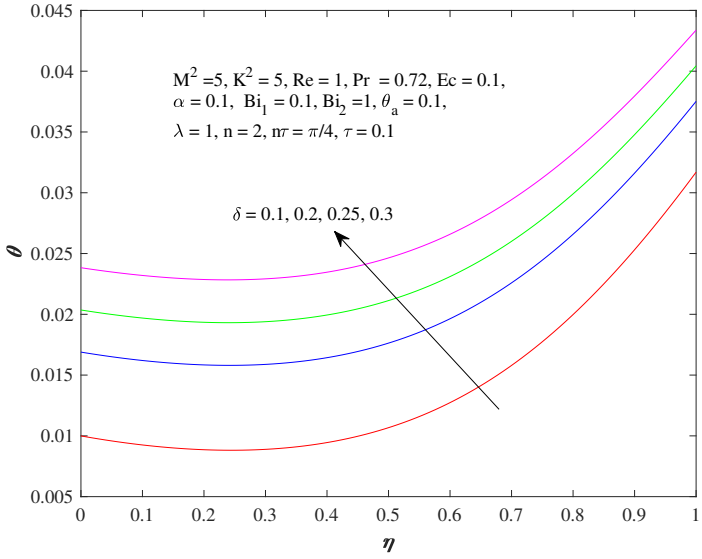

Fig.4.3(d): *Temperature profiles varying δ*

Joule electric current heating terms vanish in the energy equation. Fig.4.3(d) reveals the effects of reaction parameter δ on temperature profiles. The temperature profile is an increasing function of δ. An increase in parameter δ leads to significant increase in the reaction rate (or Arrhenius kinetic) and this increases the viscous heating source terms. As a result, the fluid temperature considerably increases. Fig.4.3(e) and 4.3(f) represent the effect of Biot number(or convective

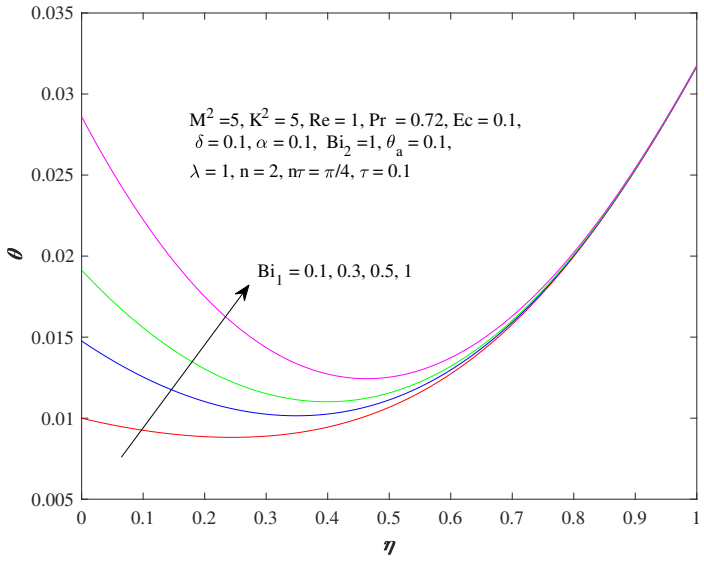

Fig.4.3(e): *Temperature profiles varying* Bi_1

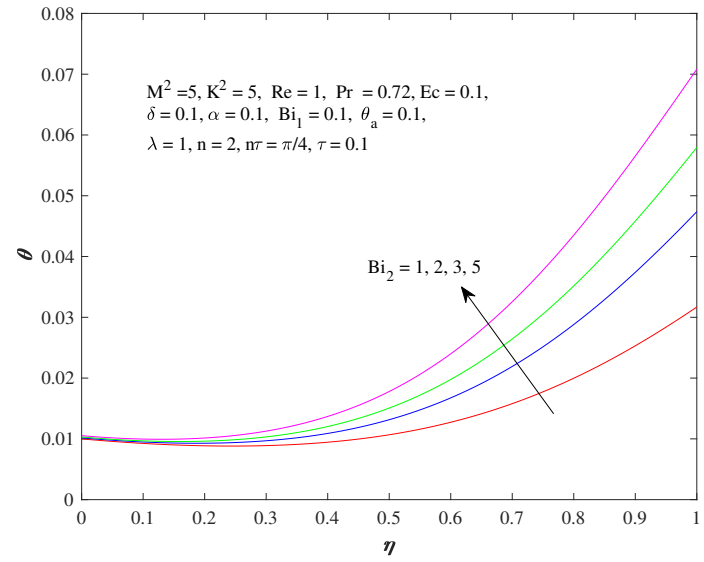

Fig.4.3(f): *Temperature profiles varying* Bi_2

heating of fluid) at both walls on temperature profiles. An increase in Biot number at both walls has increasing effect on temperature profiles within the channel. This was anticipated since the convective heating rate is increased when Biot numbers are increased, causing the temperature to elevate gradually across the channel. The maximum temperature is generally observed at both the lower and the upper plate surfaces. Fig.4.3(g) exhibits the impact of time τ on the temperature profiles. A progressive increase in temperature profiles with time τ

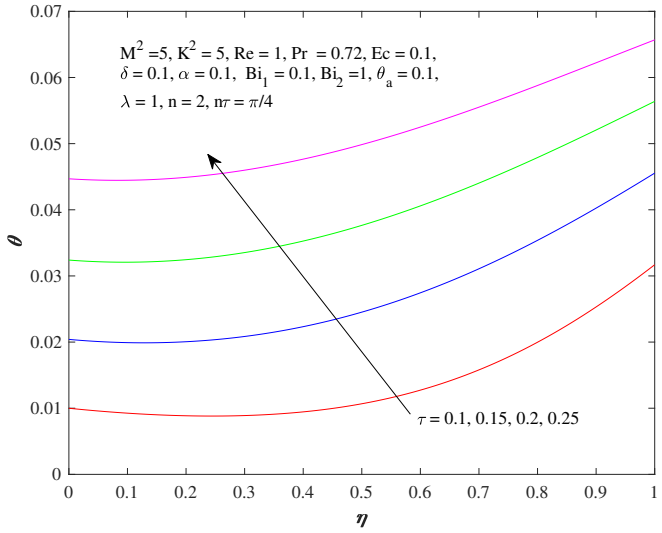

Fig.4.3(g): *Temperature profiles varying* τ

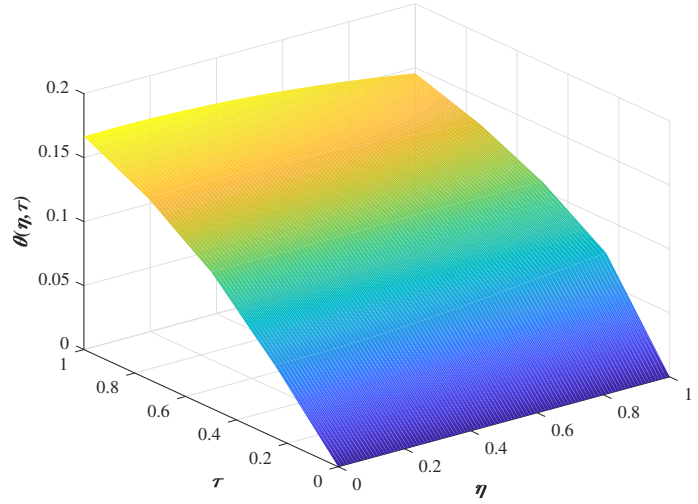

Fig.4.3(h): *Time evolution of temperature profiles varying* η *and* τ

is shown in the channel. Fig.4.3(h) gives highlights of time evolution of temperature profiles across the channel for a fixed set of parameter values from the time where the fluid is begun to flow. The temperature increases to its maximum value subject to the boundary conditions considered.

4.3.3 Shear stresses

The estimation or evaluation of wall shear stresses is important from the engineering point of view. The non-dimensional shear stresses τ_{x_0} and τ_{z_0} at the lower plate of the channel ($\eta = 0$) due to the primary and secondary flows are calculated from (4.25) and expressed as

$$\begin{aligned} \tau_{x_0} + i\tau_{z_0} &= \left(\frac{\partial q}{\partial \eta}\right)_{\eta=0} \\ &= \left(\frac{c_2\, Re}{2} + c_1\, m_1\right) + \varepsilon \left[e^{i\, n\tau}\left(\frac{c_4\, Re}{2} + c_3\, m_2\right)\right. \\ &+ \left. e^{-i\, n\tau}\left(\frac{c_6\, Re}{2} + c_5\, m_3\right)\right], \end{aligned} \tag{4.26}$$

where the expressions m_1, m_2, m_3 and $c_1, c_2, c_3, c_4, c_5, c_6$ are given in (4.24). On separating equation (4.26) into real and imaginary parts, we get the shear stress components due to the primary and secondary flows.

Numerical values of the non-dimension shear stresses τ_{x_0} and τ_{z_0} are plotted in Fig.4.4 for several values of M^2, K^2, Re, $n\tau$. Figs.4.4(a) and 4.4(b) show the

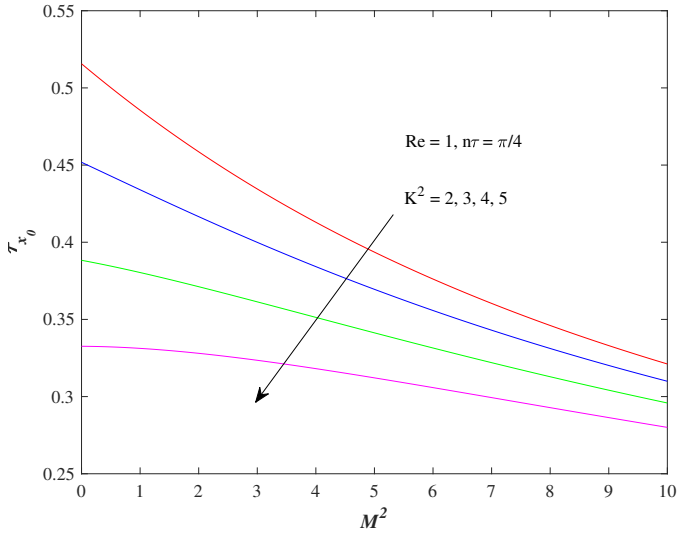

Fig.4.4(a): *Shear stress τ_{x_0} varying K^2*

effects of rotation parameter K^2 and squared-Hartmann number M^2 on the shear stresses τ_{x_0} and τ_{z_0}. The shear stress τ_{x_0} reduces whereas the shear stress τ_{z_0} enhances as K^2 increases. Both the shear stresses reduce when M^2 is increased. Increase in M^2 reduces the velocity gradient at the lower plate due to magnetic field and Lorentz force, which in turn lowers the wall shear stresses. Both the shear stresses are increasing functions of suction/injection parameter Re as shown

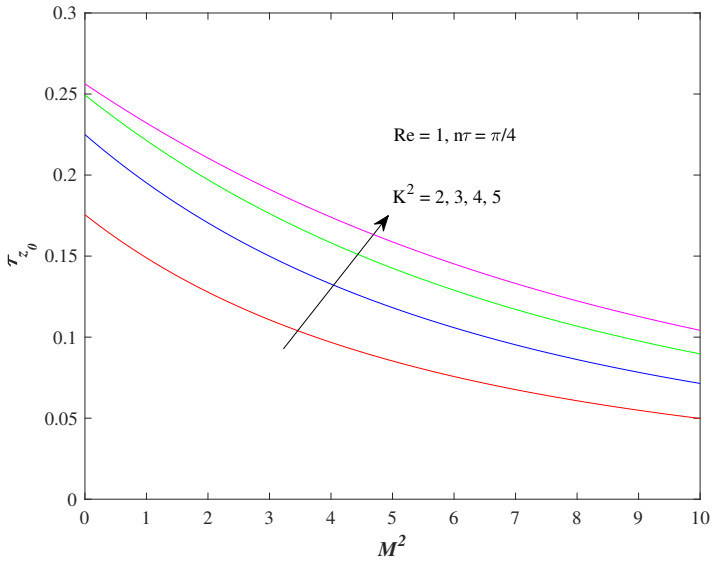

Fig.4.4(b): *Shear stress τ_{z_0} varying K^2*

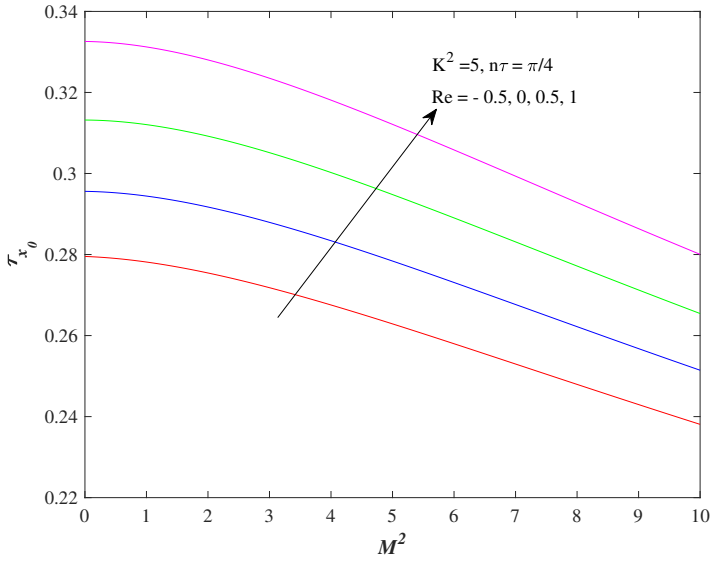

Fig.4.4(c): *Shear stress τ_{x_0} varying Re*

in Figs.4.4(c) and 4.4(d). This is related to the fact that, since the fluid motion towards the lower plate increases with increasing Re due to injection, consequently, the velocity gradient at the lower fixed plate increases, leading to an elevation of the wall shear stresses. Figs.4.4(e) and 4.4(f) show that the shear stresses τ_{x_0} and τ_{z_0} slightly decrease with increasing phase angle $n\tau$. The influence of change of phase angle on the secondary shear stress τ_{z_0} is negligible. Similarly, the shear stresses at the upper plate of the channel can be computed.

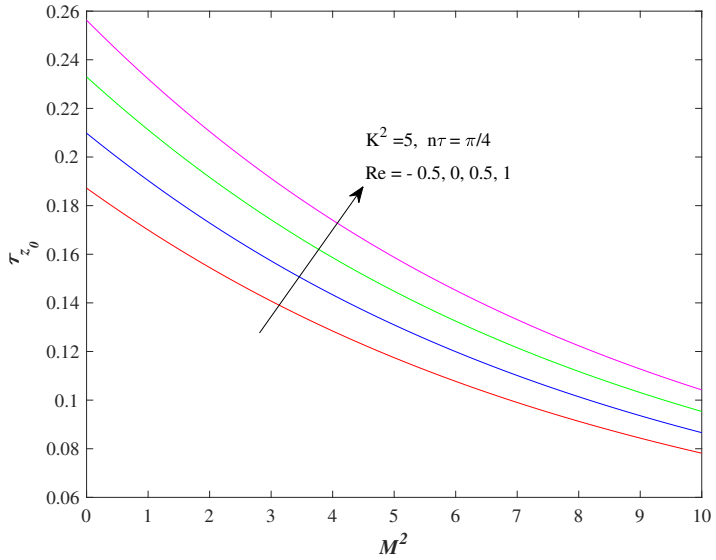

Fig.4.4(d): *Shear stress τ_{z_0} varying Re*

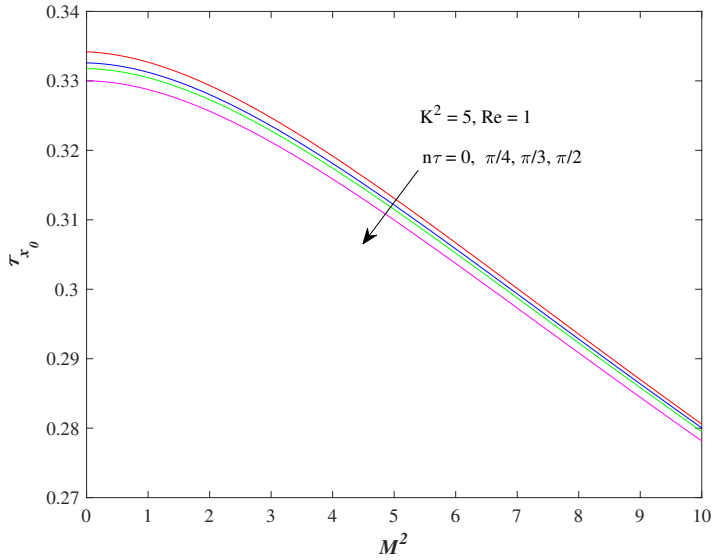

Fig.4.4(e): *Shear stress τ_{x_0} varying $n\tau$*

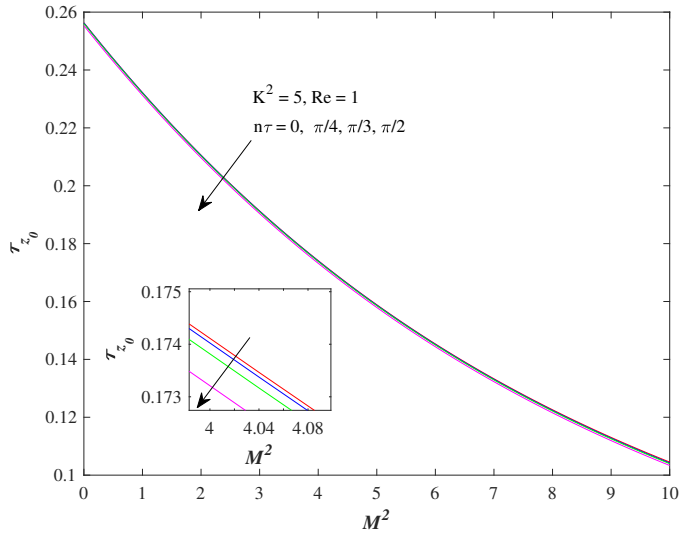

Fig.4.4(f): *Shear stress τ_{z_0} varying $n\tau$*

4.3.4 Rate of heat transfer

For practical designing purpose in MHD energy systems, one is usually interested to evaluate the values of engineering parameter, viz. the rate of heat transfer at the channel walls.

Numerical values of the rate of heat transfer $\frac{\partial\theta}{\partial\eta}\Big)_{\eta=0}$ and $\frac{\partial\theta}{\partial\eta}\Big)_{\eta=1}$ at the channel plates ($\eta = 0,\ 1$) are entered in Table 4.1 for several values of M^2, Re, δ, α, Bi_1, Bi_2, Pr, Ec, τ. Table 4.1 shows that the rate of heat transfer $\frac{\partial\theta}{\partial\eta}\Big)_{\eta=0}$ at the lower plate is increased by increasing δ or Ec or Bi_2 or τ while it decreases for increasing values of M^2 or Re or Bi_1 or Pr. The rate of heat transfer $\frac{\partial\theta}{\partial\eta}\Big)_{\eta=1}$ at the upper plate is observed to increase with increasing M^2 or Pr or Bi_2 and decreasing influence is seen for increasing values of Re or δ or Bi_1 or Ec or τ. This is expected, since temperature gradient at the upper plate decreases due to a rise in fluid suction and consequently, the heat transfer rate decreases. Increases in M^2 in the presence of suction also enhance the temperature gradient slightly at the upper plate. The rate of heat transfer at the lower plate surface increases with reaction parameter whereas it decreases at upper plate surface. This is explained by the fact that the reaction parameter increases the surface temperature leading to a reduction of the rate of heat transfer. No appreciable effect of activation parameter α on the rate of heat transfer at lower and upper plate surfaces could

Table 4.1: *The rate of heat transfer at the channel plates ($\eta = 0, 1$) when $K^2 = 5$, $\theta_a = 0.1$, $\lambda = 1$, $n = 2$, $n\tau = \pi/4$*

M^2	Re	δ	α	Bi_1	Bi_2	Pr	Ec	τ	$\frac{\partial\theta}{\partial\eta}\Big)_{\eta=0}$	$\frac{\partial\theta}{\partial\eta}\Big)_{\eta=1}$
2	1	0.1	0.1	0.1	1	0.72	0.1	0.1	−0.00900	0.06921
5	1	0.1	0.1	0.1	1	0.72	0.1	0.1	−0.00900	0.06923
10	1	0.1	0.1	0.1	1	0.72	0.1	0.1	−0.00901	0.06926
5	−0.5	0.1	0.1	0.1	1	0.72	0.1	0.1	−0.00899	0.07135
5	0	0.1	0.1	0.1	1	0.72	0.1	0.1	−0.00900	0.07066
5	1	0.1	0.1	0.1	1	0.72	0.1	0.1	−0.00900	0.06923
5	1	0.1	0.1	0.1	1	0.72	0.1	0.1	−0.00900	0.06923
5	1	0.2	0.1	0.1	1	0.72	0.1	0.1	−0.00831	0.06326
5	1	0.3	0.1	0.1	1	0.72	0.1	0.1	−0.00762	0.05723
5	1	0.1	0	0.1	1	0.72	0.1	0.1	−0.00900	0.06923
5	1	0.1	0.1	0.1	1	0.72	0.1	0.1	−0.00900	0.06923
5	1	0.1	0.2	0.1	1	0.72	0.1	0.1	−0.00900	0.06923
5	1	0.1	0.1	0.1	1	0.72	0.1	0.1	−0.00900	0.06923
5	1	0.1	0.1	0.2	1	0.72	0.1	0.1	−0.01754	0.06922
5	1	0.1	0.1	0.5	1	0.72	0.1	0.1	−0.04057	0.06917
5	1	0.1	0.1	0.1	1	0.72	0.1	0.1	−0.00900	0.06923
5	1	0.1	0.1	0.1	2	0.72	0.1	0.1	−0.00897	0.10642
5	1	0.1	0.1	0.1	3	0.72	0.1	0.1	−0.00895	0.12626
5	1	0.1	0.1	0.1	1	0.72	0.1	0.1	−0.00900	0.06923
5	1	0.1	0.1	0.1	1	1	0.1	0.1	−0.00926	0.07424
5	1	0.1	0.1	0.1	1	7.1	0.1	0.1	−0.00986	0.09369
5	1	0.1	0.1	0.1	1	0.72	0	0.1	−0.00902	0.06940
5	1	0.1	0.1	0.1	1	0.72	0.1	0.1	−0.00900	0.06923
5	1	0.1	0.1	0.1	1	0.72	0.5	0.1	−0.00898	0.06907
5	1	0.1	0.1	0.1	1	0.72	0.1	0.1	−0.00900	0.06923
5	1	0.1	0.1	0.1	1	0.72	0.1	0.2	−0.00677	0.04369
5	1	0.1	0.1	0.1	1	0.72	0.1	0.3	−0.00436	0.02587

be observed. This is due to the neglected effect of activation parameter on temperature profiles in lower and upper plate surfaces. The rate of heat transfer $\frac{\partial\theta}{\partial\eta}\Big)_{\eta=0} < 0$ means

the heat transfer take places from lower plate to the ambient fluid in the channel. On the other hand, $\frac{\partial\theta}{\partial\eta}\Big)_{\eta=0} > 0$ means the heat flows from fluid to upper plate in the channel. It is also apparent that the rate of heat transfer at the upper plate of the channel is higher. This is due to the fact that the upper plate of the channel is heated by convection from hot fluid and therefore, the upper plate surface of the channel becomes hotter. This means that heat will flow from fluid to the plate instead of plate to the fluid. Thus effective cooling of the channel can be achieved by implementing higher values of the convective heat transfer parameter.

4.4 Conclusion

This study deals with a computational investigation of the hydromagnetic oscillatory flow of a viscous incompressible electrically conducting reactive fluid through a porous channel with asymmetrical convective boundary conditions in a rotating frame of reference. The heat transfer characteristic has also been studied by taking viscous and Joule dissipations into account. The analytical expression is obtained for velocity components and use to compute the wall shear stresses. The temperature profiles and rate of heat transfer at the channel walls are computed numerically. From the study, the main findings are listed below:

- The velocity components have retarding influence with increasing values of either magnetic field or phase angle.
- The primary velocity is observed to decrease when rotation parameter is increased while the secondary velocity increases until it reaches maximum and then decreases as rotation parameter increases.
- Biot number and Eckert number increase the fluid temperature across the channel.
- A decrease in fluid temperature with increased Prandtl number while increasing reaction parameter leads to significant increase in fluid temperature within the channel.
- Reaction parameter leads to reduce the rate of heat transfer at upper plate of the channel.
- Increasing magnetic field intensity reduces wall shear stresses while increasing suction/injection Reynolds number enhances the wall shear stresses.